Transformer Internal Fault Modeling in ATP

A. Avendaño, B. A. Mork, H. K. Høidalen

***Abstract*—An important aspect to investigate when designing transformer protection schemes is the protection against internal faults. Although the accurate modeling and simulation of internal faults can be an important tool for protection engineers, there is presently no transformer model in ATP with this capability. This paper investigates on the development of transformer winding-fault models based on two different sources of information: 1) test-report data and 2) design information. Simulation results will be compared to lab measurements and conclusions regarding their accuracy shall be given.**

***Keywords*: Internal faults, transformer model, leakage reactance, finite element method, ATP/EMTP.**

I. Introduction

POWER transformers are frequently subject to a variety of electromagnetic transients during their operating lifespan. These impose stresses in windings and other components that may lead to immediate or long-term failure. Internal faults develop as a consequence of these overstresses and if left undetected, can result in high repair and replacement costs for a utility. Transformer protection relays are thus required to operate for internal faults and the accurate simulation of these can become an important tool for the development of adequate protection schemes.

Relevant work in this area has focused on building internal fault models for EMTP based on rules of consistency, leakage and proportionality applied to the faulted winding sections [1]. The method has the drawback of resorting to empirical correction factors that decrease the accuracy of the model whenever winding sections of irregular geometry are encountered or when small sections that do not reach full window height must be studied (which is usually the case). This problem can be avoided through the development of transformer models based on the Finite Element Method [2]. This may be the most accurate approach for this purpose but it requires the knowledge of detailed design information that in most cases is not readily available. A model built from only factory test-report information can be a practical alternative but its accuracy is unknown. This paper describes some practical methods for modeling internal faults according to the type of problem and amount of information available with the objective of creating a suitable model for ATP in any case. This approach works with leakage parameters directly through an admittance formulation since under load conditions the voltage and current distribution in the windings is determined by the leakage flux. The excitation characteristics were added externally through a topologically-correct duality-derived core model that includes zero-sequence inductance, making the complete transformer model suitable for transient simulations in EMTP/ATP.

In order to determine if a model based on only test-report data (which is the type of information usually available) can give acceptable results, an internal fault model was developed for a 500-kVA 11430Y/235Y V layer-layer concentric winding core-form distribution transformer using two different sources of information: 1) test-report data and 2) design information (for comparison). The main challenge here was to determine the short-circuit reactance between faulted sections using each source of information. Both modeling approaches shall be described and have been implemented in the Alternative Transients Program (ATP). Their accuracy was determined by comparing the simulated line and fault current waveforms for turn-to-ground and turn-to-turn fault conditions against laboratory measurements. Conclusions and recommendations are also given at the end of the paper.

II. Internal Fault Model

A. General Approach

The general approach for the development of the proposed models was to create a new "expanded" higher-order leakage inductance model for the transformer. The number of sections in which the windings needed to be split into depended on the type of fault to be simulated. For turn-to-ground faults, the faulted coil had to be split into two sections as seen in Fig. 1a). For turn-to-turn faults, three sections were necessary as in Fig. 1b). This allowed access to new terminals that corresponded to the position in the winding where the fault occurred and the desired connections could be made to ground or to another section of the winding.

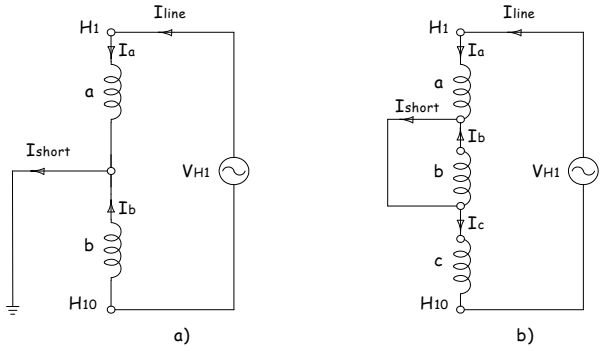

Fig. 1. Internal fault winding sections for Phase-1 of the HV-winding.

A. Avendaño and B. A. Mork are with the Department of Electrical and Computer Engineering, Michigan Technological University (MTU), Houghton, MI 49931 USA (e-mail of corresponding author: aavedano@mtu.edu).
H. K. Høidalen is with the Department of Electric Power Engineering, Norwegian University of Science and Technology (NTNU), Trondheim, Norway (e-mail: hans.hoidalen@elkraft.ntnu.no).

Paper submitted to the International Conference on Power Systems Transients (IPST2011) in Delft, the Netherlands June 14-17, 2011

Besides the simulation of the internal fault current, the model reproduced the original short-circuit behavior when the appropriate coils were connected in series.

B. Leakage Representation

Once the leakage reactances were calculated, the leakage part of the internal-fault model was represented by a winding resistance matrix $[R]$ and an inverse inductance matrix $[A]$. The matrices were created following the procedure described in [3] for the representation of single-phase N-coil transformers through an admittance formulation. This gave the well-known representation of transformers for short-circuit and power flow studies

$$[I] = [Y][V] \tag{1}$$

As recommended for transient studies, the resistive and inductive parts were separated by building $[Y]$ from the reactive part of the short-circuit data. The winding resistances then formed a diagonal matrix $[R]$, and

$$[A] = [L]^{-1} = j\omega[Y] \tag{2}$$

The extension to three-phase was made by including the zero-sequence inductance externally in the core model and by making the appropriate connections between the winding terminals. This procedure was implemented in the same manner regardless of a turn-to-ground or a turn-to-turn model. The only difference was the number of coils that needed to be represented.

III. Calculation of Leakage Reactance Between Faulted Sections

A. From Test-Report Data

Since the typical information available in a test report or transformer nameplate for this purpose is the standard short-circuit impedance, the leakage reactance between sections was calculated using only this parameter. The per-phase formulation described next is based on the splitting of the HV-winding H into N sections, denominated as windings $a, b, \dots, N$. The LV-winding L was kept as is but it can be split in a similar manner.

Consider the original transformer with an equivalent short-circuit impedance Z_{sc} (referred to the HV-side in this case) between windings H and L. An individual impedance was assigned to each winding assuming that the equivalent impedance divides equally between both in per-unit. In ohms, this gave

$$Z_H = Z_{sc}/2 \tag{3}$$

$$Z_L = Z_H/t^2 \tag{4}$$

where t is the turns ratio $t = N_H/N_L \approx V_H/V_L$ (per phase). Since the winding H had to be split into N sections, Z_H was divided proportionally according to

$$n_a = N_a/N_H \tag{5}$$

$$n_b = N_b/N_H \tag{6}$$

$$\vdots$$

$$n_N = N_N/N_H \tag{7}$$

where $N_a, N_b, \dots, N_N$ are the number of turns of each new section and are a fraction of the total number of turns N_H.

$$N_a + N_b + \cdots + N_N = N_H \tag{8}$$

$$n_a + n_b + \cdots + n_N = 1 \tag{9}$$

Calculating the individual impedance of each section,

$$Z_a = n_a Z_H \tag{10}$$

$$Z_b = n_b Z_H \tag{11}$$

$$\vdots$$

$$Z_N = n_N Z_H \tag{12}$$

The voltage for each section can also be defined:

$$V_a = n_a V_H \tag{13}$$

$$V_b = n_b V_H \tag{14}$$

$$\vdots$$

$$V_N = n_N V_H \tag{15}$$

For winding L, Z_L and V_L stay the same. The equivalent binary reactance between any two sections a and b was calculated with (16) from the imaginary parts of the respective impedances Z_a and Z_b using the corresponding turn-ratios. The real parts of (10)-(12) gave the resistance of the new windings.

$$X_{a-b} = X_a + \left(\frac{V_a}{V_b}\right)^2 X_b \tag{16}$$

The binary reactances were then converted to per-unit values using a common VA base and the corresponding base voltage of the section being referred to. From here, the method of Section II. B. was implemented to represent the terminal characteristics of the transformer for each phase.

B. From Design Information

When design information was available, the binary reactance between sections could be calculated in different ways depending on the shape and size of the new windings.

1) Rectangular Geometry, Full Window Height

When there is a uniform distribution of ampere turns between each pair of windings, the leakage flux due to the short-circuit current is predominantly axial, except at the winding ends, where there is a fringing effect due to a shorter return path for the leakage flux through the core limbs and yoke. The leakage reactance between sections could then be calculated using the common formulas for transformers with concentric windings and n flux tubes [4]:

$$X_{a-b} = 2\pi f \frac{\mu_0 \pi N^2}{H_{eq}} \sum_{k=1}^{n} ATD \tag{17}$$

$$\sum ATD = \frac{1}{3}T_a D_a + T_g D_g + \frac{1}{3}T_b D_b \tag{18}$$

$$H_{eq} = H_w / K_R \tag{19}$$

$$K_R = 1 - \frac{1 - e^{\frac{-\pi H_w}{T_a + T_g + T_b}}}{\frac{\pi H_w}{T_a + T_g + T_b}} \tag{20}$$

where ATD is the area of the Ampere-Turn Diagram, K_R is the Rogowski factor ($K_R < 1$), μ_0 is the magnetic permeability of free-space, H_w is the winding height, N is the rated number of turns of the reference side, D_a, D_g and D_b are the mean diameters and T_a, T_g and T_b are the radial depths of the first (a), gap (g), and second (b) winding, respectively. Fig. 2 shows the leakage field distribution between sections a and b when the HV-winding was split in two sections of equal height and uniformly distributed ampere-turns.

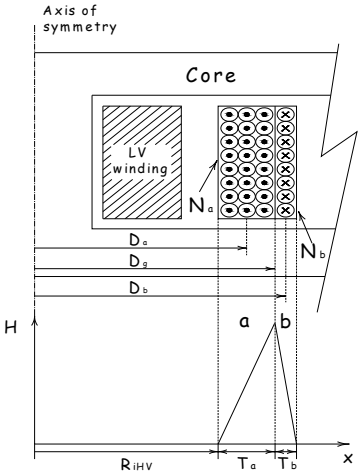

Fig. 2. Leakage magnetic field distribution between sections a and b.

2) Rectangular Geometry, Unequal Heights

When it was desired to calculate the reactance between sections of unequal ampere-turn per height distribution (e. g., when one of the sections was too small to reach full window height), the conventional formulas for concentric windings did not yield accurate results since the leakage flux was no longer predominantly axial, but had now an additional cross-flux component in the radial direction with a magnitude dependent on the degree of axial asymmetry between the sections. In this case, the reactance calculation was resolved into two separate components: one related only to the axial flux and the other depending on the radial flux component. For the first, conventional formulas for concentric windings could be used and for the second, conventional formulas for "pancake" or interleaved windings were used. The total reactance was the sum of the two reactances [4]-[6]. Referring to Fig. 3, the assymetrical winding b is replaced with windings c and d. Winding c is of equal ampere-turn per height distribution as winding a, and winding d has an ampere-turn per height distribution such that the addition of ampere-turns along the window height of c and d gives the same ampere-turns as winding b.

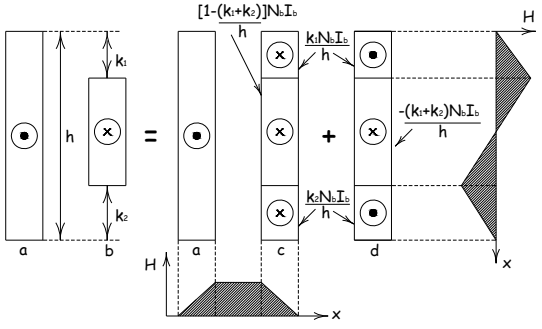

Fig. 3. Resolution of leakage magnetic field distribution for axially assymetrical windings.

3) Irregular Geometry

For cases of irregular or non-standard winding configurations, the leakage reactance could not be easily handled by classical analytical methods. The Finite Element Method (FEM) was the most suitable technique for calculating the flux distribution under these conditions. The problem could be solved through a magnetostatic study starting with Maxwell's equations for steady-current cases,

$$\nabla \mathrm{x} \mathrm{H} = \mathrm{J} \tag{21}$$

$$\nabla \cdot \mathrm{B} = 0 \tag{22}$$

where H is the magnetic field intensity, J is the current density at a point and B is the magnetic flux density. Defining the vector H for isotropic media,

$$\mathrm{H} = \mathrm{B}/\mu \tag{23}$$

where μ is the magnetic permeability of the material, then

$$\nabla \mathrm{x} \mathrm{B} = \mu \mathrm{J} \tag{24}$$

Due to (22), it should be possible to express B as

$$\mathrm{B} = \nabla \mathrm{x} \mathrm{A} \tag{25}$$

where A is the magnetic vector potential. Making

$$\nabla \cdot \mathrm{A} = 0 \tag{26}$$

A is completely defined. Taking the curl of (25), we have

$$\nabla^2 \mathrm{A} = -\mu \mathrm{J} \tag{27}$$

which is Poisson's equation for the vector potential and is the general form of the equation solved by commercial FEM software. Once a solution for the vector potential was obtained, the instantaneous energy W_i stored in winding i could be calculated by evaluating (28) only over the volume of the winding

$$W_i = \frac{1}{2}\int_{vol} J_i \cdot A dv \tag{28}$$

The total magnetic energy W_T was given by the sum of the energy stored in each winding. Alternatively, the total magnetic energy stored in the steady field over the volume of the core window could be calculated by

$$W_T = \frac{1}{2}\int_{vol} B \cdot H dv \tag{29}$$

The total magnetic energy then defined the total leakage inductance referred to any one specific winding

$$L = 2W_T / I_i^2 \tag{30}$$

where I_i is the nominal current of winding i.

IV. Adding The Core Model

The core representation generated by the Hybrid Transformer Model [8] was implemented in ATPDraw using open-circuit test data at different excitation levels as an input to an XFMR model for the 500-kVA transformer. The core-loss resistance, current, and flux linked values were acquired from the .lis file of the XFMR circuit and were input into resistive, linear, and nonlinear inductive elements as shown in Fig. 4. Z_l and Z_y represent the nonlinear limbs and yokes respectively, and L_4 represents the zero-sequence path through the tank.

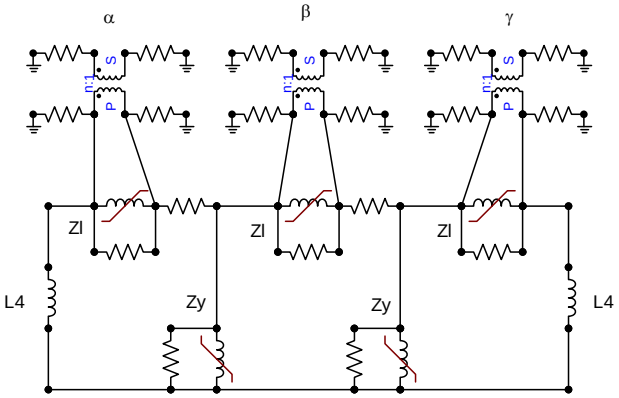

Fig. 4. Core attached to N+1[th] winding.

The attachment of the core to the leakage model was made through ideal transformers of unity-turns ratio representing the α, β, γ terminals of an infinitely-thin N+1[th] "coil" at the surface of the core leg C. The reactance between the core and the primary and secondary coils was estimated as in [8], [9]. For the case of a two-winding transformer with concentric windings,

$$X_{LC} \approx 0.5 X_{HL} \tag{31}$$

$$X_{HC} \approx 2 X_{HL} \tag{32}$$

Since the primary or secondary windings had to be split into sub-coils to simulate internal faults, the procedure of Section III. A. was applied to the values of (31) and (32) to calculate the reactance between sections and the core winding.

V. Internal-Fault Study

Internal-fault laboratory tests were made to benchmark the simulations using the available taps on the HV-winding. Fig. 5 is a schematic of the HV-coil which consisted of 8 1/2 layers and ±2x2.5% taps (shaded regions). Sections a and b for the turn-to-ground fault study are also shown. The HV-winding was energized with a reduced 3-phase voltage for cases where the LV-winding was both open- and short-circuited. With the appropriate connections, turn-to-ground faults were applied on one phase at a time, where the bottom 5% of the coil was shorted. Turn-to-turn faults were applied in a similar manner, where the point corresponding to 5% of the coil was shorted to another corresponding to 2.5%.

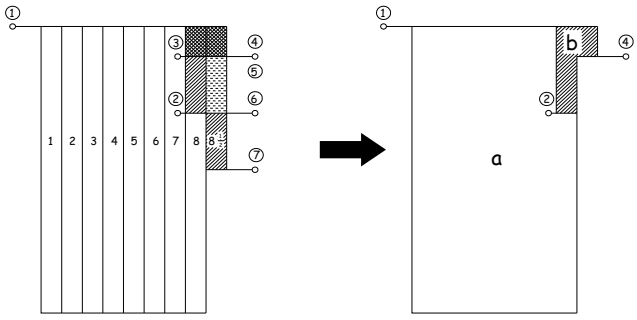

Fig. 5. HV-winding tap and layer arrangement, 500-kVA transformer.

A. Modeling Approach

Since the geometry of the faulted sections was of irregular shape, a 2D-FEM model was created using COMSOL for the outer leg of the transformer in order to calculate the leakage reactance between sections. A model that uses only test-report data as an input was also created for comparison. The influence of the core was included in the FEM simulations with a core model that represented the total core reluctance seen from the outer leg [10]. Since it was an axisymmetric model, the yoke height varied along the radial direction to give a constant yoke area. The core-to-coil reactances were calculated using (31) and (32). After all the reactances were calculated, the procedure of Section II. B. was followed to create a leakage description for ATP where the [A] and [R] matrices were input through a user-specified library component. The connection between the fictitious winding and duality-derived core model was made by referencing the α, β, γ nodes of the ideal transformers of Fig. 4 in [A]. Fig. 6 shows the complete model implemented in ATPDraw with a turn-to-ground fault being simulated on Phase-A of the HV-winding while the LV-winding was short-circuited.

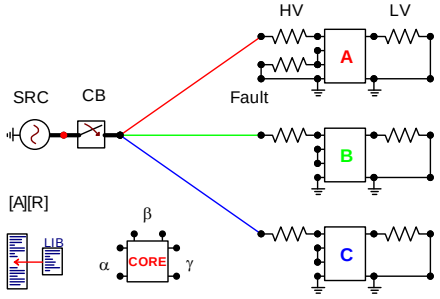

Fig. 6. Internal–fault model implemented in ATPDraw.

VI. Results

A. Short-Circuit Reactance

Table I shows the measured and calculated per-phase reactance values between sections *a, b* (95 and 5% of the HV-coil, respectively), and the LV-coil *L* given by the two models. The results show that the approach where the Finite Element Method is used along with (30) yields much closer results to the measurements than by using (16). The typical short-circuit reactance given in a test report or nameplate is measured under balanced, steady-state conditions. Although the values calculated using the test-report approach represent an exact higher-order equivalent circuit of the windings, the actual leakage flux path under fault conditions is not being adequately represented.

TABLE I
CALCULATED REACTANCE VALUES BETWEEN COIL SECTIONS FROM TEST-REPORT AND DESIGN DATA MODELS (Ω REFERRED TO TEST WINDING).

Reactance	Measured	Test-Report Model	$\%e_{T\text{-}REP}$	FEM Model	$\%e_{FEM}$
X_a-L	8.86	9.617	8.54	8.71	-1.69
X_a-b	58.56	98.63	68.42	56.48	-3.55
X_b-L	0.187	0.2725	45.72	0.1774	-5.13

Comparing the calculated values using the FEM model and (30) with previous measurements, the maximum percent error magnitude encountered was of 5.13%. The differences in values can be due to the fact that in the FEM model the complete winding cross-section was considered as a solid current-carrying conductor but in reality there is insulation between turns that decreases the conducting area, which in turn increases the current density of each winding, resulting in a larger magnetic energy that would yield a higher leakage inductance. Additional sources of error can be due to the omission of the winding lead that connects to the HV-bushing, manufacturing tolerances, and small measurement errors.

B. Simulation of Internal Faults-FEM Model

Fig. 7 shows a plot of the line and fault currents of Phase-A when the bottom 5% of the HV-winding was shorted to ground. There is a slight phase-error of 4.5° due to the difference between measured and modeled impedances but overall the simulation shows good agreement with the measurements. Table II shows more simulation results for 5% turn-to-ground and 5-2.5% turn-to-turn faults (LV-coils open and short-circuited).

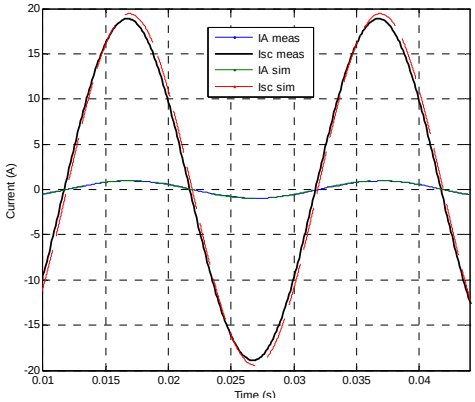

Fig. 7. Internal fault 5%-to-ground, LV open-circuited, 500-kVA transformer.

TABLE II
BENCHMARKING OF LINE AND INTERNAL FAULT CURRENTS (PEAK A)

Test	IA Meas	IA Sim	%e IA	Isc Meas	Isc Sim	%e Isc
T-G_oc	0.96	0.98	2.08	18.89	19.42	2.8
T-G_sc	14.65	14.74	0.61	19.62	20.93	6.67
T-T_oc	0.51	.55	7.84	18.99	19.94	5.0
T-T_sc	6.54	6.67	1.98	20.19	21.19	4.95

Fig. 8 shows the magnetic flux density in the window area during a 5% turn-to-ground internal fault. Fig. 9 shows the magnetic vector potential contour during a 5-2.5% turn-to-turn fault where a large radial component can be observed. In both plots the LV-winding is open-circuited.

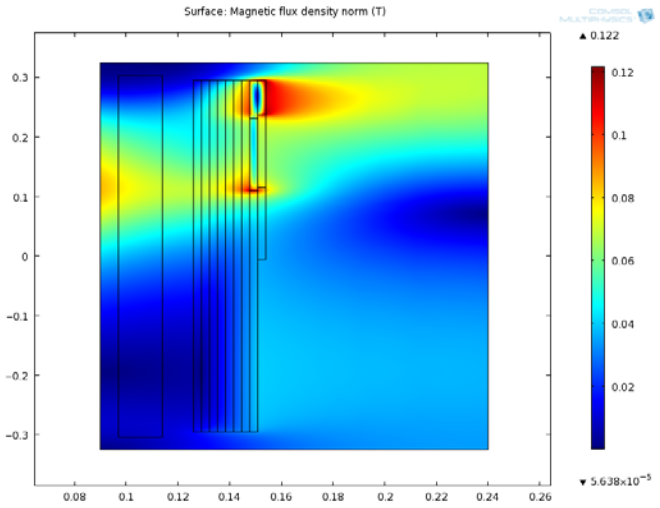

Fig. 8. Magnetic flux density, 5% turn-to-ground fault, LV open-circuited.

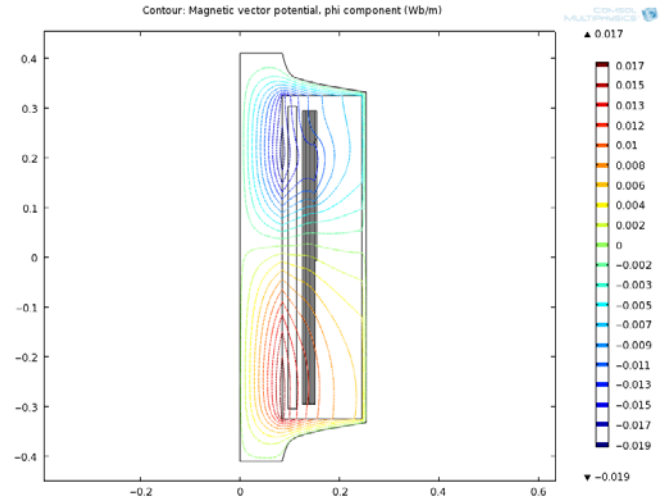

Fig. 9. Vector potential, 5-2.5% turn-to-turn fault, LV open-circuited.

VII. Conclusions

In this work, internal fault models built from factory test-report and design information were developed and their accuracy was compared. It was determined that the calculation of leakage reactance between faulted winding sections was more accurate when a FEM model was constructed using design information. A maximum error magnitude of 5.13% was obtained with this approach, giving internal fault simulations with a maximum error magnitude of 7.84% in the

currents. This error considerably grew when using only the 2-winding short circuit impedance to create a higher-order leakage model for the transformer under study. This last model did not accurately represent the internal short-circuit behavior of the transformer since the leakage reactance between faulted sections (determining the line and fault currents) depends not only on the number of short-circuited turns, but also on their geometry and position in the winding. Since this needs to be taken into account, design information is thus necessary for its accurate calculation.

VIII. Future Work

An investigation of internal faults on additional transformers of different size and configuration shall be made in order to better evaluate the test-report data model.

Since design information defining winding dimensions is already a source of information for the Hybrid Transformer Model in ATPDraw, the methods described in Sections III. B. 1) and III. B. 2) could be implemented in the XFMR to simulate internal faults when the resulting sections are of rectangular geometry.

For irregular winding geometries, a 3-D FEM model can be investigated in order to improve accuracy. An analytical formulation could also be implemented as an alternative to a FEM model but with some simplifications in order to facilitate the analysis of the problem [12]-[14]. Some of these are the assumption of infinite permeability of the core, negligible effects of ducts and insulation in windings, and that the sum of ampere-turns between windings is always zero. A comparison with FEM calculations could be made to investigate its accuracy.

IX. References

[1] P. Bastard, P. Bertrand, M. Meunier, "A transformer model for winding fault studies," *IEEE Trans. Power Del.*, vol. 9, no. 2, pp. 690-699, Apr. 1994.

[2] H. Wang, K. L. Butler, "Finite element analysis of internal winding faults in distribution transformers," *IEEE Trans. Power Del.*, vol. 16, no. 3, Jul. 2001.

[3] V. Brandwajn, H. W. Dommel, I. I. Dommel, "Matrix representation of three-phase N-winding transformers for steady-state and transient studies," *IEEE Trans. Power App. Syst.*, vol. PAS-101, no. 6, pp. 1369-1375, Jun. 1982.

[4] S.V. Kulkarni, S.A. Khaparde, *Transformer Engineering Design and Practice*, New York, NY: Marcel Dekker, Inc., 2004.

[5] H. O. Stephens, "Transformer reactance and losses with nonuniform windings," *Electrical Engineering*, vol. 53, pp. 346-49, Feb. 1934.

[6] A. K. Sawhney, *A Course in Electrical Machine Design*, Delhi, India: Dhanpat Rai & Sons, 1994.

[7] S. Jamali, M. Ardebili, K. Abbaszadeh, "Calculation of short circuit reactance and electromagnetic forces in three phase transformer by finite element method," *Proc. 8th Int. Conf. on Electrical Machines and Systems*, vol. 3, pp. 1725-1730, Sept. 2005.

[8] B.A. Mork, F. Gonzalez, D. Ishchenko, D. L. Stuehm, J. Mitra, "Hybrid transformer model for transient simulation-Part I: Development and parameters," *IEEE Trans. Power Del.*, vol. 22, pp. 248-255, Jan. 2007.

[9] B.A. Mork, F. Gonzalez, and D. Ishchenko, "Leakage inductance model for autotransformer transient simulation," presented at the International Conference on Power System Transients, Montreal, Canada, 2005. [Online]. Available: http://www.ipst.org/IPST05Papers.htm.

[10] E. Bjerkan, "High frequency modeling of power transformers - Stresses and diagnostics," Doctoral Thesis, Norwegian University of Science and Technology, Trondheim, Norway, 2005.

[11] H. W. Dommel, *Electromagnetic Transients Program Reference Manual (EMTP Theory Book)*, Portland, OR, Prepared for BPA, Aug. 1986.

[12] E. Billig, "The calculation of the magnetic field of rectangular conductors in a closed slot, and its application to the reactance of transformer windings," *Proc. IEE-Part IV: Institution Monographs*, vol. 98, no. 1, pp. 55-64, 1951.

[13] A. Boyajian, "Leakage reactance of irregular distributions of transformer windings by the method of double Fourier series," *AIEE Trans. Power App. Syst.*, vol. 73, Pt. III, pp. 1078-1086, Oct., 1954.

[14] L. Rabins, "Transformer reactance calculations with digital computers," *AIEE Trans. Power App. Syst.*, vol. 75, pt. 1, pp. 261-267, 1956.

X. Biographies

Alejandro Avendaño was born in Tijuana, México, on January 19, 1982. He received the B.S. degree in Electromechanical Engineering from Instituto Tecnológico de Tjuana in 2004. In 2005 he was awarded with a scholarship from the National Research Council of Mexico (CONACYT) and joined the Department of Electric & Computer Engineering at Michigan Technological University. He is now a Ph.D. candidate at MTU.

Bruce A. Mork (M'82) was born in Bismarck, ND, on June 4, 1957. He received the BSME, MSEE, and Ph.D. (Electrical Engineering) from North Dakota State University in 1979, 1981 and 1992 respectively.
From 1982 through 1986 he worked as design engineer for Burns and McDonnell Engineering in Kansas City, MO, in the areas of substation design, protective relaying, and communications. He has spent 3 years in Norway: 1989-90 as research engineer for the Norwegian State Power Board in Oslo; 1990-91 as visiting researcher at the Norwegian Institute of Technology in Trondheim; 2001-02 as visiting Senior Scientist at SINTEF Energy Research, Trondheim. He joined the faculty of Michigan Technological University in 1992, where he is now Professor of Electrical Engineering, and Director of the Power & Energy Research Center.

Hans K. Høidalen was born in Norway in 1967. He received his MSc and PhD from the Norwegian University of Science and Technology in 1990 and 1998 respectively. He is now a professor at the same institution with a special interest of electrical stress calculations and modeling.